

Whispering-gallery-mode resonators as frequency references. II. Stabilization

Anatoliy A. Savchenkov, Andrey B. Matsko,* Vladimir S. Ilchenko, Nan Yu, and Lute Maleki

Jet Propulsion Laboratory, California Institute of Technology, 4800 Oak Grove Drive, Pasadena, California 91109-8099, USA

**Corresponding author: Andrey.Matsko@jpl.nasa.gov*

Received August 16, 2007; accepted September 20, 2007;
posted October 11, 2007 (Doc. ID 86538); published November 14, 2007

We show theoretically that the absolute frequency stability of a solid-state millimeter-scale whispering gallery mode resonator can reach one part per 10^{-14} per 1 s integration time if proper crystalline material as well as proper stabilization technique is selected. Both the fluctuations of the resonator temperature and the fluctuations of the temperature in the mode volume can be measured with the sensitivity better than the fundamental thermodynamic limit and actively compensated. © 2007 Optical Society of America

OCIS codes: 230.5750, 120.6810, 350.5340.

1. INTRODUCTION

Ultrastable optical resonators play an important role in both classical and quantum optics [1–14], and generally are of Fabry–Perot (FP) type. They are fabricated from materials having ultralow thermal expansion coefficients, and are both thermally and mechanically isolated to achieve stability. The geometrical dimensions of these types of resonators are typically ~ 10 cm or larger. Lasers locked to such resonators demonstrate hertz and even subhertz linewidth, with frequency stabilities as high as $\sim 10^{-15}$ at 1 s.

A new class of ultra-high- Q optical whispering gallery mode (WGM) resonators (see [15–22] for review) is more attractive than FP resonators if compactness or miniaturization matters. Fabrication and handling of the WGM resonators, even crystalline ones, is relatively simple [23,24], and efficient coupling techniques with prisms [25,26], side-polished fiber couplers [27], fiber tapers [28,29], and angle-polished fiber tips [30] have been demonstrated. The spectra of WGMs can be modified by changing the morphology of the resonators [31,32]. Nonlinear WGM resonators can be used as optical and microwave oscillators. Handling such resonators is easier compared with handling FP resonators containing nonlinear materials. Moreover, nonlinear processes are efficient in WGM resonators because of small geometrical volumes occupied by WGMs [33–36].

With these properties, WGM resonators are naturally attractive for frequency stabilization of lasers as well as for fabrication of other kinds of frequency references. Preliminary experiments with stabilization of two diode lasers with a fused silica microsphere have been performed [37]. The result of that work was not very impressive compared with the best results of laser frequency stabilization using FP resonators since (i) the microsphere was not temperature stabilized, (ii) light coupling into and out of the microsphere was not stabilized, and (iii) relative drift

of the laser frequency resulting from the fluctuations of the driving currents was not stabilized.

The fundamental limits of WGM frequency stability were studied in our previous paper [38]. We showed that the stability of a passively stabilized millimeter-sized WGM resonator made of a certain class of crystalline materials is determined primarily by thermorefractive fluctuations. Those fluctuations have been predicted and successfully observed in fused silica microspheres [39]. The frequency stability limit of a cylindrical WGM resonator having $100\ \mu\text{m}$ in thickness and several millimeters in diameter is of the order of one part in 10^{-12} at 1 s integration time [38]. Thermorefractive fluctuations increase inversely proportional to the mode volume, and the predicted stability is limited because of small volumes of the WGMs.

The basic message of this contribution is that a proper selection of the resonator host material is essential for the stabilization of the WGM frequency. Photorefractive fluctuations can be suppressed in some materials, such as magnesium fluoride, if a proper operation temperature is selected. Thermal expansion fluctuations become dominant in the frequency stability limit in those resonators. This is a new result compared with the predictions made in [38,39]. We also show here that using specific inhomogeneous thermal expansion properties of some crystals it is possible to design methods of further active stabilization of the fluctuations of the resonator frequency resulting from the residual thermal expansion fluctuations. The achieved frequency stability could be better than the stability determined by the fundamental thermodynamic limit.

In the rest of this paper we discuss methods of realizing the desired frequency stability. We show that the simple passive temperature stabilization is not practical because it must sustain temperature fluctuations smaller than sub-micro-kelvin level. To solve this problem we make use

of methods similar to the technologies developed for the stabilization of quartz crystalline radio frequency (RF) oscillators [40]. The scheme includes (i) compensation of the temperature drifts of the resonator by connecting it with special elements having given linear or nonlinear thermal expansion (cf. oven-controlled crystal RF oscillator) and (ii) usage of two WGM families having different thermo-optical constants for measurement and compensation of the resonator temperature fluctuations. The methods can be very efficient. It is argued that the relative stability of two WGMs separated by an octave can be better than one part per 10^{-14} at 1 s integration time.

This paper is organized as follows. We consider the thermodynamic limits of frequency stability of WGM resonators made of various crystalline materials and find the related Allan variance in Section 2. In Section 3 we describe a method of stabilization of WGM frequency that allows suppressing both thermorefractive and thermal expansion fluctuations. In Appendixes A–C, we describe various technical methods of passive and active stabilization of the resonator frequency, as was promised in the first paper of the series [38]. Engineering of thermal response of the resonator is discussed in Appendix A. Various frequency stabilization schemes that are based on conventional thermal stabilization methods are discussed in Appendix B. In Appendix C we describe frequency stabilization methods that require at least two WGMs belonging to different mode families, without any additional temperature sensor.

2. ENGINEERING THERMAL RESPONSE OF THE RESONATOR: THE ROLE OF THE HOST MATERIAL

Suppression of the external temperature fluctuations is important for reaching the fundamental thermodynamic limit of WGM frequency stability. One of the basic disadvantages of WGM resonators is the large thermorefractive coefficient, as well as thermal expansion coefficient, of the majority of transparent optical materials from which resonators are usually made. Because the light entering a WGM resonator is always confined within the dielectric material, and not in vacuum, even a small temperature change results in a large frequency shift of the

WGMs. This phenomenon leads, for instance, to thermal bistability in high- Q WGM resonators [23,41–43].

Let us consider the properties of several transparent materials (see Table 1) and find the external temperature stabilization required for achieving thermodynamically limited frequency stability of resonators made out of those materials. We consider bare resonators at this point.

We use the following expressions to estimate the frequency stability

$$\frac{\langle(\Delta\omega_{TR})^2\rangle}{\omega^2} = \alpha_n^2 \frac{k_B T^2}{C V_m \rho}, \quad (1)$$

$$\frac{\langle(\Delta\omega_{TE1})^2\rangle}{\omega^2} = \alpha_l^2 \frac{k_B T^2}{C V_r \rho}, \quad (2)$$

$$\frac{\langle(\Delta\omega_{TE2})^2\rangle}{\omega^2} = k_B T \frac{\beta_T}{9V_r}, \quad (3)$$

where $\Delta\omega_{TR}$, $\Delta\omega_{TE1}$, and $\Delta\omega_{TE2}$ are the frequency deviations due to thermorefractive, thermal expansion, and thermoelastic fluctuations, respectively; k_B is the Boltzmann's constant; T is the absolute temperature; ρ is the density of the resonator host material; C is the specific heat capacity; n is the refractive index; $\alpha_n = (1/n)(\partial n/\partial T)$ is the thermorefractive coefficient; $\alpha_l = (1/l)(\partial l/\partial T)$ is the linear thermal expansion coefficient; κ is the thermal conductivity coefficient; $\beta_T = -[(1/V)(\partial V/\partial p)]_T$ is the compressibility of the resonator host material; and V_m and V_r are the volumes of the mode and the resonator, respectively. Physically Eqs. (1)–(3) describe square deviation of a mode frequency from the center of frequency distributions resulting from the corresponding thermodynamic processes. To study the deviations given by Eqs. (1)–(3) experimentally one needs to measure the frequency of a WGM instantaneously, to create the statistical distribution of the measurement results, and to find the square deviation of the frequency characterizing the distribution.

To estimate the required quality of the compensation of the external temperature fluctuations that would allow reaching the thermodynamic limit we set $\Delta T = \langle(\Delta\omega)^2\rangle^{1/2}/[\omega(\alpha_n + \alpha_l)]$. The idea is that the influence of

Table 1. Linear and Nonlinear Thermorefractive Coefficients of the Ca, Ba, MgF₂, Sapphire, and Crystalline Quartz at $T=300$ K and $\lambda=1.5$ μm^a

Material	α_n (10^{-6} K ⁻¹)	α_l (10^{-6} K ⁻¹)	n	ρ (g/cm ³)	C , [10^6 erg/(g K)]	κ [10^5 erg/(cm s K)]	β_T (10^{-12} cm ² /dyn)
CaF ₂	−8.0 [44]	18.9 [45]	1.4261 [44]	3.18 [46]	8.54 [47,48]	9.7 [48,49]	1.1 [50]
BaF ₂	−11.0 [45]	18.7 [45]	1.4662 [45]	4.83	4.56 [51]	7.1 [52]	1.5 [53]
MgF ₂ (e)	0.25 [54,55]	13.0 [56]	1.38341 [57]	3.18 [56]	9.2 [47]	30 [58]	1.0
MgF ₂ (o)	0.6 [54,55]	9.0 [56]	1.37191 [57]	3.18 [56]	9.2 [47]	21 [58]	1.0
Al ₂ O ₂ (e)	7.5 [59]	8.1 [60]	1.7384 [59]	3.98 [61]	7.61 [61]	25.2	0.4
Al ₂ O ₃ (o)	7.4 [59]	7.3 [60]	1.7462 [59]	3.98 [61]	7.61 [61]	24.1	0.4
SiO ₂ (e)	−6.8 [62]	7.6 [63]	1.5363 [64]	2.65 [63]	7.41	11.7 [58]	2.7
SiO ₂ (o)	−5.2 [62]	13.9 [63]	1.5278 [64]	2.65 [63]	7.41	6.5 [58]	2.7

^aThe data are taken from manufacturer specifications if the reference is not provided. We should note that the values vary significantly depending on the published study and/or the specifications. The variation: reaches tens of percents. We use the following notations: ρ is the density, C is the specific heat capacity (we assume that $C_p=C_v=C$), n is the refractive index, $\alpha_n=(1/n)(\partial n/\partial T)$ is the thermorefractive coefficient, $\alpha_l=(1/l)(\partial l/\partial T)$ is the linear thermal expansion coefficient, κ is the thermal conductivity coefficient, $\beta_T = -[(1/V)(\partial V/\partial p)]_T$ is the compressibility of the resonator host material (we assume that the isothermal and adiabatic compressibilities are approximately equal).

Table 2. Thermorefractive, Thermal Expansion, and Thermoelastic of WGM Frequency Stability at Room Temperature^a

Material	$\langle(\Delta\omega_{TR})^2\rangle^{1/2}/\omega$	ΔT_{TR} (nK)	$\langle(\Delta\omega_{TE1})^2\rangle^{1/2}/\omega$	ΔT_{TE1} (nK)	$\langle(\Delta\omega_{TE2})^2\rangle^{1/2}/\omega$	ΔT_{TE2} (nK)
CaF ₂	2.2×10^{-12}	80	2.4×10^{-13}	9	2.4×10^{-12}	89
BaF ₂	3.3×10^{-12}	427	2.6×10^{-13}	34	3.4×10^{-12}	446
MgF ₂	6.5×10^{-14}	7	1.1×10^{-13}	11	2.3×10^{-12}	246
Al ₂ O ₃	1.9×10^{-22}	129	8.8×10^{-14}	6	1.6×10^{-12}	109
SiO ₂	2.2×10^{-12}	303	2.1×10^{-13}	29	3.4×10^{-12}	481

^a ΔT ; determines the effective value of external temperature instability (quality of compensation of external technical temperature fluctuations) required to observe the limits.

the external temperature fluctuations can be relaxed if thermorefractive effect compensates thermal expansion. For anisotropic materials we (i) consider WGM resonators with symmetry axis coinciding with the crystalline axis, (ii) consider WGMs polarized along the crystalline axis (TE modes), (iii) select ordinary α_l and extraordinary α_n . Overall, such an estimate is valid if temperature gradients due to external temperature variations are small within the resonator. The results are shown in Table 2.

It is easy to find that the external temperature stabilization of the whole system should be at least on the level of 0.1 μ K at 1 s to achieve the frequency stability given by the thermodynamic limit. The stabilization should be even better for materials with low thermorefractive constant, such as magnesium fluoride. Realization of such a level of stabilization is a challenging task. We discuss possible approaches for relaxing this requirement in the following sections.

A. Thermorefractive Fluctuations

The basic source of the fundamental long-term (the integration time exceeds or is equal to 1 s) WGM frequency instability comes from the thermorefractive fluctuations if one considers calcium fluoride, sapphire, or quartz resonators [38]. The spectral density of the thermorefractive frequency noise could be estimated from

$$S_{\delta\omega/\omega}(\Omega) \approx \frac{k_B \alpha_n^2 T^2}{\rho C V_m} \frac{R^2}{12D} \left[1 + \left(\frac{R^2 |\Omega|}{D 9\sqrt{3}} \right)^{3/2} + \frac{1}{6} \left(\frac{R^2 \Omega}{D 8\nu^{1/3}} \right)^2 \right]^{-1}. \quad (4)$$

This equation is valid for a thin cylindrical resonator of thickness L and radius R ($R \gg L$), α_n is the thermorefractive coefficient of the material, V_m is the volume of the WGM mode, $\nu = 2\pi Rn/\lambda$ is the mode order, n is the refractive index of the material, $D = \kappa/(\rho C)$ is the temperature diffusion coefficient, κ is the thermal conductivity coefficient, and C is the specific heat capacity.

We find the Allan variance of the WGM frequency by integrating the evaluated spectral density of the fluctuations using the expression from [65]

$$\sigma^2(\tau) = \frac{2}{\pi} \int_0^\infty S_{\delta\omega/\omega}(\Omega) \frac{\sin^4(\Omega\tau/2)}{(\Omega\tau/2)^2} d\Omega, \quad (5)$$

where we took into account that $S_{\delta\omega/\omega}(\Omega)$ is a double-sided spectral density.

We consider a calcium fluoride resonator of radius $R = 0.3$ cm and thickness $L = 0.01$ cm driven with $\lambda = 1.55$ μ m light. We find $\nu = 2\pi Rn/\lambda \approx 2.7 \times 10^4$ and $R/\nu^{2/3} \approx 1.1 \times 10^{-3}$. The thermal diffusivity for calcium fluoride is equal to $D = 3.6 \times 10^{-2}$ cm²/s, hence characteristic frequencies for the process are $D/R^2 = 0.4$ s⁻¹, $D\nu^{4/3}/R^2 = 3.2 \times 10^5$ s⁻¹, and $D/L^2 = 360$ s⁻¹. To find the factor $k_B \alpha_n^2 T^2 / \rho C V_m \approx 4 \times 10^{-24}$ we have taken $\alpha_n = -0.8 \times 10^{-5}$ K⁻¹, and $V_m = 2\pi R L \times R/\nu^{2/3} \approx 6 \times 10^{-6}$ cm³. The evaluated Allan variance for the resonator is shown in Fig. 1.

To understand the change of the slope of the dependence shown in Fig. 1 we note that the integration (averaging) in Eq. (5) occurs in the vicinity of $\Omega = 0$ when $\tau \rightarrow \infty$, where spectral density [Eq. (4)] is approximately constant and $\sigma^2(\tau) \sim 1/\tau$. In the case of $\tau \rightarrow 0$ the integration in Eq. (5) occurs in a wideband centered at frequency $\Omega \rightarrow \infty$, so that $S_{\delta\omega/\omega}(\Omega) \sim 1/\Omega^2$ and $\sigma^2(\tau) \sim \tau$. The monotonic function $\sigma^2(\tau)$ naturally has a maximum at some specific value of τ . Increase of the Allan variance with time for small τ is not counterintuitive because the thermorefractive fluctuations result in the thermal drift of the WGM frequency. The maximum value of the drift is restricted and longer integration results in the averaging down of the fluctuations.

An advantage of crystalline WGM resonators compared with other solid-state resonators is that the WGM resonators can be made out of various materials with various thermorefractive constants. For instance, it is important to mention the unique properties of magnesium fluoride. The dependence of the refractive index of the material on temperature is shown in Fig. 2. This crystal has a vanish-

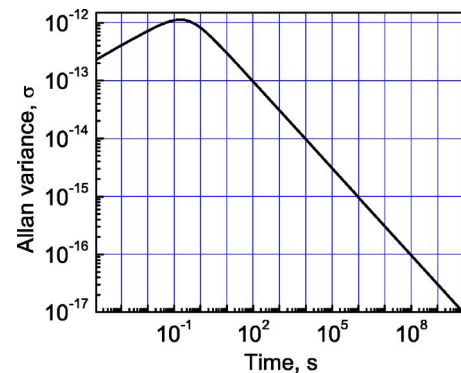


Fig. 1. (Color online) Thermorefractive Allan variance of the frequency of a mode of a cylindrical calcium fluoride WGM resonator with $R = 0.3$ cm and $L = 0.01$ cm.

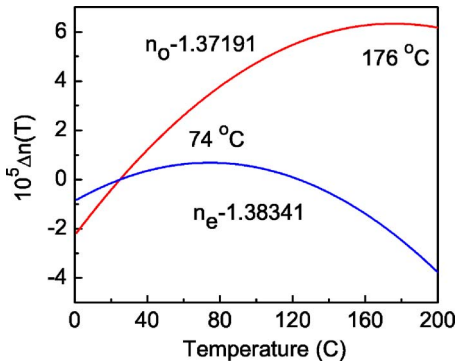


Fig. 2. (Color online) Temperature dependence of the thermorefractive deviation of the ordinary ($n_o = \Delta n + 1.37191$) and extraordinary ($n_e = \Delta n + 1.38341$) indexes of refraction of magnesium fluoride at $1.55 \mu\text{m}$. The dependencies are obtained using expressions $\partial n_e / \partial T = [0.04183 - 5.63233 \times 10^{-4} T] \times 10^{-5}$ and $\partial n_o / \partial T = [0.09797 - 5.57293 \times 10^{-4} T] \times 10^{-5}$ found from measurement data [54].

ing extraordinary (at $\sim 74^\circ\text{C}$) and ordinary (at $\sim 176^\circ\text{C}$) thermorefractive coefficients [45] given by slope of the curves shown in Fig. 2. Tuning the temperature of a magnesium fluoride WGM resonator to the vicinity of zero thermorefractive coefficient $\alpha_n = 0$ allows one to suppress the fundamental thermorefractive noise $\langle (\Delta\omega_{TR})^2 \rangle^{1/2} / \omega \rightarrow 0$. Technical thermorefractive noise is also compensated because temperature stability of the order of 2 mK required to reach $\Delta n_e / n_e = 10^{-14}$ is feasible.

The basic conclusion of this section is that the thermorefractive noise does not limit the stability of WGM resonators made out of certain materials even with moderate temperature stabilization and no sophisticated compensation. However, the other noise sources have to be dealt with to reach higher stability.

B. Fluctuations Due to Thermal Expansion

We have neglected the fluctuations of the WGM frequency resulting from the thermal expansion of the resonator in our previous paper [38] arguing that the fluctuations are generally much smaller than the thermorefractive ones. However, in the case of vanishing thermorefractive fluctuations we have to take the thermal expansion into account.

Let us first consider the fundamental fluctuations. Thermodynamic temperature fluctuations of the resonator result in the modification of the resonator radius and thickness leading to WGM frequency noise. To estimate this noise we assume that the basic contribution comes from the lowest-order eigenfunction of the thermal diffusion equation. Using the reasoning of [38] for the noise spectral density we derive

$$S_{\delta\omega/\omega} = \frac{\langle (\Delta\omega_{TE1})^2 \rangle}{\omega^2} \frac{2R^2/\pi^2 D}{1 + (\Omega R^2/D\pi^2)^2}. \quad (6)$$

This expression basically tells us that the frequency dependence of the spectral density is determined by the slowest thermal diffusion time associated with the thermal diffusion along the radius of the resonator. Using Eq. (5) we calculate the Allan variance of the frequency of the WGM resulting from the fundamental thermal expansion fluctuations of a z -cut magnesium fluoride resonator of ra-

dius $R = 0.3 \text{ cm}$ and thickness $L = 0.01 \text{ cm}$ (Fig. 3). The thermal diffusivity for magnesium fluoride is equal to $D = 7.2 \times 10^{-2} \text{ cm}^2/\text{s}$ and the characteristic frequency for the process is $D/R^2 = 0.8 \text{ s}^{-1}$. Equation (6) gives the top boundary of the low-frequency spectral density.

In reality, the resonator can be placed on a metal plate possessing a high thermal conductivity, so eventually the time constant $R^2/\pi^2 D$ should be replaced with $L^2/\pi^2 D$; this would reduce the value of the low-frequency spectral density significantly. For example, the thermal diffusivity of aluminum is $D = 0.97 \text{ cm}^2/\text{s}$ at 300 K. Copper has a bit bigger value: $D = 1.15 \text{ cm}^2/\text{s}$ at 300 K. Placing the resonator on a polished copper plate (or squeezing the resonator between two copper plates) would result in more than an order of magnitude reduction of phase noise at zero frequency leading to a reduction of the corresponding Allan variance below one part per 10^{-14} at 1 s integration time. It is important to note that placing a resonator onto a copper plate will reduce the quality factor of the mechanical modes of the resonator. This reduction will lead to enhancement of the influence of thermoelastic fluctuations on the frequency stability.

We find the solution to the problem in the optimal shaping of the resonator allowing to increase the resonator volume without changing the characteristic time constant of the process. The resonator should have a nearly spherical shape or the shape of a cylinder with equal radius and height. The light should travel in a small protrusion [31] that does not influence the thermal and mechanical modes of the resonator. For instance, a nearly spherical single mode magnesium fluoride WGM resonator of radius $R = 0.3 \text{ cm}$ will have an Allan variance less than one part per 10^{-14} at 1 s integration time. This improvement will not increase the thermoelastic fluctuations.

C. Thermoelastic Fluctuations

Almost all the related values in Table 2 look comparable. However, the thermoelastic part $\Delta\omega_{TE2}$ comes from the mechanical oscillations of the resonator. Those oscillations have high frequencies and do not significantly modify the Allan variance of the WGM frequency for 1 s and longer integration times. The thermodynamically limited Allan variance for the frequency of a WGM of a magnesium fluoride resonator is shown in Fig. 4. We expect that the technical thermoelastic fluctuations are not an issue either; given its small size it is relatively easy to isolate the resonator from external mechanical influences.

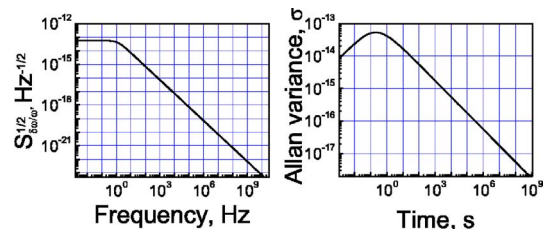


Fig. 3. (Color online) Power spectral density and Allan variance of the thermal expansion defined frequency fluctuations of a mode of a cylindrical magnesium fluoride WGM resonator with $R = 0.3 \text{ cm}$ and $L = 0.01 \text{ cm}$.

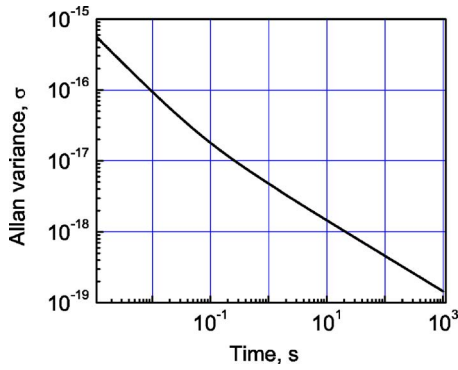


Fig. 4. (Color online) Allan variance of the thermoelastic frequency fluctuations of a mode of a cylindrical magnesium fluoride WGM resonator with $R=0.3$ cm and $L=0.01$ cm.

3. TRIPLE-MODE FREQUENCY STABILIZATION

We have shown that it is fundamentally possible to reach high-frequency stability of WGMs properly selecting the operating conditions along with the host material as well as the morphology of the resonators. We discuss technical issues of frequency stabilization of such resonators in Appendixes A–C. The only stabilization method we would like to highlight in the main part of the paper is a “triple-mode” technique. This technique is purely photonic and it enables stabilization of the WGM frequency better than the fundamental thermodynamic limit.

We propose to use three WGMs to suppress both thermorefractive and thermal expansion noise. Let us consider a spherical magnesium fluoride resonator with crystalline axis corresponding to the Z axis of a coordinate frame. The resonator is kept at 176°C where modes polarized perpendicularly to the Z axis have a negligible thermorefractive effect. We propose to excite TM mode in the XY plane and TE mode in the XZ plane. Both these modes have identical vanishing thermorefractive. A comparison of the frequency difference between these modes ($\omega_{\text{RF}} + \Delta\tilde{\omega}_{\text{RF2}}$) with the frequency of RF clocks gives averaged resonator temperature because

$$\Delta\tilde{\omega}_{\text{RF2}} \sim \omega(\alpha_{l_o} - \alpha_{l_e})\Delta T_R, \quad (7)$$

where $\Delta\tilde{\omega}_{\text{RF2}}$ is the variation of the frequency difference between two modes determined by the temperature fluctuations of the resonator, ω is the optical frequency, and α_{l_o} (α_{l_e}) is the thermal expansion coefficient for X and Y (Z) directions. The third mode, TE, is excited in the XY plane. The frequency difference between this mode and the TM mode in the same plane contains information about the temperature in the WGM channel [Eq. (C1)]. Both modes are influenced by the thermal expansion in the same way. Using results of the temperature measurements one creates a proper feedback and/or compensation scheme (see Appendixes A–C) that results in suppression of both thermorefractive and thermal expansion fluctuations for the TM mode family in the XY plane. The relative stability of those modes is determined by expression

$$\frac{\Delta\omega_{\text{TM}}}{\omega} \sim \frac{\alpha_{l_o}}{\alpha_{l_o} - \alpha_{l_e}} \frac{\Delta\tilde{\omega}_{\text{RF2}}}{\omega}. \quad (8)$$

It is possible to achieve $\Delta\omega_{\text{TM}} \sim \tilde{\omega}_{\text{RF2}}$ if $\alpha_{l_o} \neq \alpha_{l_e}$.

It is also possible to measure the resonator temperature with sensitivity better than the fundamental thermodynamic limit. The measurement sensitivity is limited by value $\Delta\tilde{\omega}_{\text{RF2}}/[\omega(\alpha_{l_o} - \alpha_{l_e})]$, which can be very small if $\Delta\tilde{\omega}_{\text{RF2}}$ is small enough. Hence, the triple-mode technique results in a possibility of compensation of the thermodynamic noises better than the fundamental thermodynamic limit. There is nothing special in the suppression of the fundamental thermorefractive frequency fluctuations of an optical mode if one manages to lock this mode to an ultrastable optical frequency reference. The advantage of the proposed technique is in the possibility to stabilize optical frequency beyond the thermodynamic limit using a RF reference. This feature will result in creation of stable UV as well as FIR lasers using crystalline WGM resonators.

4. CONCLUSION

The importance of a proper selection of the WGM resonator host material for achieving high-frequency stability is elucidated. Various frequency stabilization techniques applicable to whispering gallery mode resonators are discussed. It is shown that it is possible to stabilize optical WGM resonators using external RF references such that the resultant absolute WGM stability approaches the RF clock stability. Finally, it is shown that the stabilization technique also results in temperature measurement of the WGM resonators with sensitivity better than the fundamental thermodynamic limit. The stabilization technique described in this study can be considered as one more step toward realization of the standard quantum limit of frequency stability of an oscillator [66,67].

APPENDIX A: COMPENSATION OF TECHNICAL THERMAL FLUCTUATIONS

Stabilization of the WGM frequency requires controlling the thermal response of the resonator to reduce unwanted averaged frequency drifts. In this Appendix we describe several methods for such a control via passive stabilization of the average frequency of WGMs.

1. Linear Compensation

The basic goal of compensation techniques, including the linear compensation, is in the suppression of technical noise resulting from the temperature fluctuations of the entire setup. The compensation allows relaxing the requirements for temperature stabilization, but does not influence the fundamental thermodynamic limits of the frequency stability. An example of such a linear compensation arrangement is discussed below and the corresponding setup is shown in Fig. 5.

The resonator (3) is placed into the setup consisting from a rigid frame (1) and a spacer (2) with different thermal expansion coefficients. The sandwiched resonator is made much thinner than the frame and spacer. In this way, thermal expansion of the resonator does not result in any significant stress of the spacer and the frame, so the stress forces in the system are determined by those parts only. The frame has a much larger cross section than the spacer to generate a much stronger force than the spacer

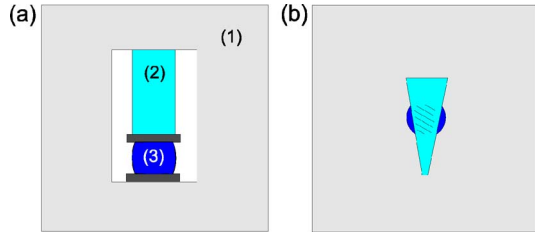


Fig. 5. (Color online) (a) Thermal compensator for an optical WGM resonator. The compensator consists of (1) a rigid metal frame with thermal expansion coefficient α_1 ; (2) a metal or a glass wedge-shaped spacer with thermal expansion coefficient α_2 ; and (3) a WGM resonator sandwiched between rigid spacers on its top and bottom. (b) Top view of the wedge part of the thermal compensator. The dashed zone is an effective overlap cross section \mathcal{A}_2 of spacer (2) and resonator (3). The cross-section area can be tuned continuously with high precision by shifting the spacer up and down with respect to spacer position shown in the picture.

during the entire range of thermally induced expansion or contraction. Thus, the expansion of the spacer is determined by the expansion of the frame only. The force applied to the sandwiched disk is $\mathcal{A}_2 E_2 (\alpha_2 - \alpha_1) \Delta T$, where \mathcal{A}_2 is the cross section of the spacer and the resonator, E_2 is the stress modulus of the spacer, α_1 is the thermal expansion coefficient of the frame, and α_2 is the thermal expansion coefficient of the spacer.

The resonator has a thermally induced frequency tunability $d\omega/dT = (\alpha_n + \alpha_l)\omega$ and stress induced tunability $d\omega/dF$. The frequency drift of the free resonator is determined by $d\omega/dT$. With applied stress the total frequency drift is

$$\Delta\omega = \left[(\alpha_n + \alpha_l)\omega + \frac{d\omega}{dF} \mathcal{A}_2 E_2 (\alpha_2 - \alpha_1) \right] \Delta T. \quad (\text{A1})$$

The thermal frequency drift is compensated if $\Delta\omega/\Delta T = 0$. The values of $d\omega/dT$ and $d\omega/dF$ can be inferred from experimental measurements. They depend on the host material and the shape of the resonator. The cross-section area of the spacer (2) and the resonator are free parameters here. The spacer should have, e.g., a wedgelike shape [Fig. 5(b)] for adjusting \mathcal{A}_2 . Various other compensators of different shapes can be designed based on this principle.

2. High-Order Compensation

It is technically difficult to select parameter \mathcal{A}_2 to compensate the thermal WGM frequency drift exactly. Unavoidable errors of the mechanical manufacturing of the compensator elements will lead to an incomplete compensation of the frequency drift. For that reason we introduce a nonlinear element (4) and the oven (5) (Fig. 6). The nonlinear element shrinks nonlinearly under stress so the force exposed to the sandwiched resonator depends on temperature as $\mathcal{A}_2 E_2 (\alpha_2 - \alpha_1) \Delta T + A (\Delta T)^2$, where the factor A depends on the structure and shape of the nonlinear element. To describe a nonlinear compensation Eq. (A1) should be modified as

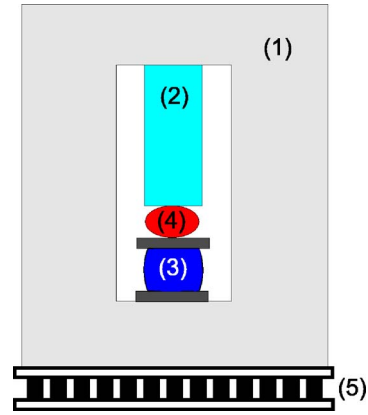


Fig. 6. (Color online) Nonlinear thermal compensator for an optical WGM resonator. An enhanced temperature compensation compared with the compensation realized in the linear device (Fig. 5) is achieved by shifting of the working point towards both the first- and the second-order compensation temperature region. The temperature tuning is realized with heater (5). The nonlinearity is introduced by nonlinear element (4).

$$\Delta\omega = \left\{ (\alpha_n + \alpha_l)\omega + \frac{d\omega}{dF} [\mathcal{A}_2 E_2 (\alpha_2 - \alpha_1) + A \Delta T] \right\} \Delta T. \quad (\text{A2})$$

The nonlinear frequency shift controlled by an oven allows fixing the incomplete compensation inevitable in the linear version of the compensator. The compensator can potentially reduce the required nanoKelvin level temperature stabilization accuracy by several orders of magnitude making it feasible.

APPENDIX B: ACTIVE STABILIZATION

We have considered methods of passive compensation-stabilization of the resonator frequency in Appendix A. In this Appendix we consider active stabilization methods. The temperature of the resonator is monitored by a single (or several) thermally sensitive elements attached to the resonator surface. The techniques considered here can be used for suppressing the frequency fluctuations due to technical, not fundamental, temperature drifts. Using the analogy with quartz oscillators, we propose three basic methods for active stabilization of the WGM frequency shown in Fig. 7.

These methods have the following distinctive features. In the scheme with temperature compensated resonator the temperature of the resonator oscillates freely. The frequency stability is obtained using a temperature independent phenomena. In the scheme of oven-controlled resonator the temperature of the whole system is stabilized. Finally, in the scheme involving microprocessor stabilization the frequency of the WGMs is tuned using an additional resonator, and the WGM resonator is not disturbed. It is clear that a combination of the techniques can give better frequency stability as compared with the results achieved with each particular method.

The basic disadvantage of the stabilization methods considered above is in the relatively low temperature stability of the reference included into the temperature measurement device. The whole system should be tempera-

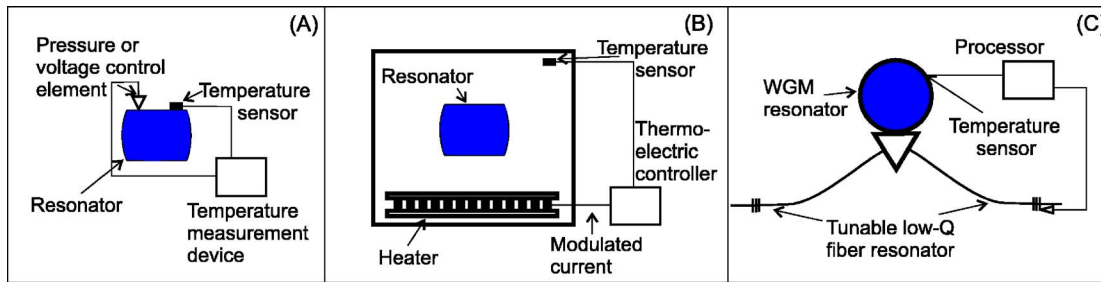


Fig. 7. (Color online) (a) Temperature compensated WGM resonator. The overall temperature of the resonator is kept higher than the room temperature. The output signal from a temperature sensor with an internal temperature reference is used to feed forward to a pressure actuator. The output signal can also be transferred to a voltage signal that changes the WGM frequency (if the resonator is made of quartz or other electro-optic material). (b) Oven controlled WGM resonator. The WGM resonator and other temperature sensitive components are in a temperature stabilized oven that is kept at a temperature where the WGM frequency has zero slope versus the oven temperature $d\omega/dT=0$ (temperature feedback). (c) Microprocessor compensated WGM resonator. Temperature of the WGM resonator is measured and inserted into a smart optical element (low-Q resonator) that compensates for the frequency shift of the WGM. The optical element should memorize the dependence of the WGM frequency on the temperature.

ture compensated by itself to reach the required nanoKelvin/second stability. Reaching such a stability is not that difficult and has been realized in many laboratories. However it is not so practical for general applications because it requires a good thermal isolation as well as high precision temperature sensors. Materials such as magnesium fluoride allow creating better stabilization systems as discussed in Appendix C.

APPENDIX C: DUAL-MODE STABILIZATION

The dual-mode stabilization is an example of the active stabilization technique. The basic idea of the dual-mode frequency stabilization is to measure the temperature of the resonator using the resonator modes themselves, without use of an external temperature sensor. Frequency difference between two WGMs having different thermorefractive coefficient should be compared with relatively stable RF frequency and the resultant signal should be used for both temperature measurement and temperature compensation. The temperature measurement is also possible if one uses two optical WGMs separated by an octave. An advantage of the dual-mode stabilization technique is its ability to monitor the temperature of the material inside the WGM channel. External sensors show local temperatures and are unable to get such information. The technique cannot generally be efficiently applied to the thermal expansion noise, so it should be integrated with another similar stabilization technique that involves the three modes discussed in Section 3 of the paper.

1. RF Frequency Referenced Technique

a. Thermorefractive Noise

The method of stabilization is applicable to a WGM resonator made of a birefringent medium. The resonator is interrogated with coherent light polarized 45° with respect to the polarization of both the ordinary and extraordinary modes of the resonator. The light is modulated by a tunable RF source. The horizontally polarized component of the light is fed into an ordinarily polarized WGM. The carrier frequency of the laser is locked at the center of the mode. A sideband of the modulated light is fed into and locked to an arbitrary selected extraordinarily polarized

mode. It is possible to use two independent lasers locked to two differently polarized modes instead of the single laser and the modulator. The modulation frequency (or the beating frequency of the two lasers) becomes a measure of the frequency difference between the ordinarily and extraordinarily polarized modes. Change of the temperature ΔT_m in the WGM channel results in frequency shift $\Delta\omega_{RF}$ of the RF frequency by

$$\Delta\omega_{RF1} = \omega(\alpha_{no} - \alpha_{ne})\Delta T_m, \quad (C1)$$

where ω is the optical frequency, and α_{no} (α_{ne}) is the thermorefractive coefficient for ordinarily (extraordinarily) polarized light.

Let us estimate the frequency shifts for a z -cut magnesium fluoride resonator interrogated with $1.55 \mu\text{m}$ light ($\omega = 1.2 \times 10^{15}$ rad/s), and assume that the resonator is kept at 74°C , when $\alpha_{ne} = 0$ and $\alpha_{no} \approx 4 \times 10^{-7} \text{ K}^{-1}$. We find $\Delta\omega_{RF1}/2\pi = 80\Delta T_m$ MHz. Monitoring the RF frequency with a modest accuracy of ~ 1 kHz per 1 s and subsequently actively stabilizing the temperature results in a significant (better than one part per 10^{-14} per 1 s integration time) suppression of the thermorefractive frequency fluctuations for the TE mode. The monitoring is simple because the spectral width of WGMs should not exceed several kilohertz for $Q > 10^{10}$ (no mode overlap). Therefore, dual-mode frequency stabilization results in a significant suppression of the photorefractive frequency noise.

The measurement accuracy of the temperature deviation inside the WGM channel can be very high. A simple locking technique is capable of determining the center of the line of a WGM with much better precision than the width of the resonance. For instance, a laser locked to a several kilohertz linewidth WGM can have frequency deviation relatively to the WGM less than 0.1 Hz per 1 s integration time. A good quartz oscillator can have 1 MHz carrier frequency with Allan variance of 10^{-7} at 1 s integration time. The measurement of $\Delta\omega_{RF1}$ using the laser and the oscillator gives an ability to monitor the mode channel temperature fluctuations with an accuracy exceeding 1 nK at 1 s integration time.

The accuracy is limited by the incomplete mode overlap and cross-phase modulation noise. An incomplete mode overlap results in somewhat uncorrelated temperature

fluctuations for the TE and TM WGMs. This effect is not important if the measurement occurs in the vicinity of the point of zero thermal refractivity for any of the modes. The measurement primarily gives information about the temperature within the channel of the mode with nonzero thermorefractive coefficient. The effect of the cross-phase modulation is of the same order of magnitude as the effect of self-phase modulation, which is negligibly small [38].

b. Thermal Expansion Noise

Thermal expansion results in nearly identical drift of both TE and TM modes. The relative drifts of the optical frequency as well as the frequency separation between two modes are identical. The overall expansion of the resonator due to a change of the averaged temperature (ΔT_R) results in a frequency shift between any two WGMs separated by frequency ω_{RF} given by

$$\Delta\omega_{RF2} \simeq \omega_{RF}\alpha_l\Delta T_R. \quad (C2)$$

It is easy to find that $\Delta\omega_{RF2}/2\pi \simeq 10\Delta T_R$ for a *z*-cut magnesium fluoride resonator with $\omega_{RF}/2\pi = 1$ MHz. This drift is small compared with the thermorefractive drift $\Delta\omega_{RF1}$. It is very difficult to compensate for the random thermal expansion using information on TE–TM frequency detuning.

The thermal expansion fluctuations can be suppressed by increasing the thermal conductivity of the setup. Unfortunately the thermal expansion related noise is eliminated only if the thermal conductivity becomes infinitely large. The more conventional way is to compensate for the random deviation of the optical frequency using error signal generated by two optical modes with substantially different thermal expansion coefficients, similar to the dual-mode technique described above. This approach is described in Section 3.

The geometrical approach of compensation for linear expansion is rather labor consuming. An advantage of using WGM resonators for frequency stabilization is the ability to manufacture the resonators practically out of any optically transparent crystal. Novel materials of zero thermal expansion can provide a much simpler conventional dual-mode technique of frequency stabilization. It is known that there are crystals with negative and zero thermal expansion at some specific temperature [68–70]. Doping changes the properties of these crystals. Hence, it is not impossible to create an optically transparent crystal with zero thermal expansion at room temperature. Application of the stabilization technique discussed above will result in the creation of a WGM resonator possessing an extremely high-frequency stability.

In principle, the dual-mode technique allows for frequency stabilization better than the thermodynamic frequency limit for the both thermorefractive and thermal expansion fluctuations. This is possible in a ring resonator made of a thin crystalline wire where the WGM volume coincides with the volume of the resonator. However, technical implementation of such a resonator is problematic.

2. Technique Based on Frequency Doubling

This technique can be used for stabilization of the temperature inside the WGM channel for resonators made

out of symmetric materials. Here modes with different polarizations and the same frequency have the same thermorefractive coefficient α_n , but the coefficient itself is frequency dependent. Consider a WGM resonator interacting with bichromatic light having frequency ω and $\Delta\omega_{RF} + 2\omega$. A laser with carrier frequency ω is locked to a mode. Then the second-harmonic light is produced by frequency doubling in a nonlinear crystal and it is subsequently frequency shifted with an acousto-optical modulator. The frequency shift $\Delta\omega_{RF}$ is locked to another WGM and is compared with a RF reference. The value of $\Delta\omega_{RF}$ fluctuates due to thermorefractive effect. The fluctuation is described by

$$\Delta\tilde{\omega}_{RF1} = 2\omega(\alpha_n(\omega) - \alpha_n(2\omega))\Delta T_m, \quad (C3)$$

and can be used for measurement of T_m . Because the relative accuracy of measurement of $\Delta\tilde{\omega}_{RF1}$ can easily reach the subhertz level, the relative frequency of the two WGMs separated by an octave can be stabilized better than one part per 10^{-14} per 1 s integration time.

ACKNOWLEDGMENTS

The research described in this paper was carried out at the Jet Propulsion Laboratory, California Institute of Technology, under a contract with the National Aeronautics and Space Administration, and with support from the Defense Advanced Research Projects Agency (DARPA). A. Savchenkov and A. Matsko gratefully acknowledge useful discussions with Dmitry Strekalov.

REFERENCES

1. R. W. P. Drever, J. L. Hall, F. V. Kowalski, J. Hough, G. M. Ford, A. J. Munley, and H. Ward, "Laser phase and frequency stabilization using an optical resonator," *Appl. Phys. B* **31**, 97–105 (1983).
2. Ch. Salomon, D. Hils, and J. L. Hall, "Laser stabilization at the millihertz level," *J. Opt. Soc. Am. B* **5**, 1576–1587 (1988).
3. T. Day, E. K. Gustafson, and R. L. Byer, "Sub-Hertz relative frequency stabilization of 2-diode laser-pumped Nd:YAG lasers locked to a Fabry–Perot interferometer," *IEEE J. Quantum Electron.* **28**, 1106–1117 (1992).
4. J. Dirscherl, B. Neizert, T. Wegener, and H. Walther, "A dye laser spectrometer for high resolution spectroscopy," *Opt. Commun.* **91**, 131–139 (1992).
5. S. Seel, R. Storz, G. Ruoso, J. Mlynek, and S. Schiller, "Cryogenic optical resonators: a new tool for laser frequency stabilization at the 1 Hz level," *Phys. Rev. Lett.* **78**, 4741–4744 (1997).
6. B. C. Young, F. C. Cruz, W. M. Itano, and J. C. Bergquist, "Visible lasers with subhertz linewidths," *Phys. Rev. Lett.* **82**, 3799–3802 (1999).
7. M. Eichenseer, A. Yu. Nevsky, Ch. Schwedes, J. von Zanthier, and H. Walther, "Towards an indium single-ion optical frequency standard," *J. Phys. B* **36**, 553–559 (2003).
8. S. A. Webster, M. Oxborrow, and P. Gill, "Subhertz-linewidth Nd:YAG laser," *Opt. Lett.* **29**, 1497–1499 (2004).
9. K. Numata, A. Kemery, and J. Camp, "Thermal-noise limit in the frequency stabilization of lasers with rigid cavities," *Phys. Rev. Lett.* **93**, 250602 (2004).
10. M. Notcutt, L.-S. Ma, J. Ye, and J. L. Hall, "Simple and compact 1-Hz laser system via an improved mounting

- configuration of a reference cavity," *Opt. Lett.* **30**, 1815–1817 (2005).
11. T. Nazarova, F. Riehle, and U. Sterr, "Vibration-insensitive reference cavity for an ultra-narrow-linewidth laser," *Appl. Phys. B* **83**, 531–536 (2006).
 12. H. Stoehr, F. Mensing, J. Helmcke, and U. Sterr, "Diode laser with 1 Hz linewidth," *Opt. Lett.* **31**, 736–738 (2006).
 13. S. A. Webster, M. Oxborrow, and P. Gill, "Vibration insensitive optical cavity," *Phys. Rev. A* **75**, 011801 (2007).
 14. A. D. Ludlow, X. Huang, M. Notcutt, T. Zanon-Willette, S. M. Foreman, M. M. Boyd, S. Blatt, and J. Ye, "Compact, thermal-noise-limited optical cavity for diode laser stabilization at 1×10^{-15} ," *Opt. Lett.* **32**, 641–643 (2007).
 15. P. W. Barber and R. K. Chang, eds., *Optical Effects Associated with Small Particles* (World Scientific, 1988).
 16. R. K. Chang and A. J. Campillo, eds., *Optical Processes in Microcavities*, Vol. 3 of Advanced Series in Applied Physics (World Scientific, 1996).
 17. M. H. Fields, J. Popp, and R. K. Chang, "Nonlinear optics in microspheres," *Prog. Opt.* **41**, 1–95 (2000).
 18. V. V. Datsyuk and I. A. Izmailov, "Optics of microdroplets," *Usp. Fiz. Nauk* **171**, 1117–1129 (2001) [*Phys. Usp.* **44**, 1061–1073 (2001)].
 19. A. N. Oraevsky, "Whispering-gallery waves," *Quantum Electron.* **32**, 377–400 (2002).
 20. K. J. Vahala, "Optical microcavities," *Nature* **424**, 839–846 (2003).
 21. A. B. Matsko and V. S. Ilchenko, "Optical resonators with whispering gallery modes I: basics," *IEEE J. Sel. Top. Quantum Electron.* **12**, 3–14 (2006).
 22. V. S. Ilchenko and A. B. Matsko, "Optical resonators with whispering gallery modes II: applications," *IEEE J. Sel. Top. Quantum Electron.* **12**, 15–32 (2006).
 23. A. A. Savchenkov, V. S. Ilchenko, A. B. Matsko, and L. Maleki, "Kilohertz optical resonances in dielectric crystal cavities," *Phys. Rev. A* **70**, 051804R (2004).
 24. I. S. Grudin, A. Savchenkov, A. B. Matsko, D. Strekalov, V. Ilchenko, and L. Maleki, "Ultra high Q crystalline microcavities," *Opt. Commun.* **265**, 33–38 (2006).
 25. S. Shiller and R. L. Byer, "High-resolution spectroscopy of whispering gallery modes in large dielectric spheres," *Opt. Lett.* **16**, 130–132 (1991).
 26. M. L. Gorodetsky and V. S. Ilchenko, "Optical microsphere resonators: optimal coupling to high- Q whispering-gallery modes," *J. Opt. Soc. Am. B* **16**, 147–154 (1999).
 27. A. Serpenguzel, S. Arnold, and G. Griffel, "Excitation of resonances of microspheres on an optical fiber," *Opt. Lett.* **20**, 654–656 (1994).
 28. J. C. Knight, G. Cheung, F. Jacques, and T. A. Birks, "Phase-matched excitation of whispering gallery mode resonances using a fiber taper," *Opt. Lett.* **22**, 1129–1131 (1997).
 29. S. M. Spillane, T. J. Kippenberg, O. J. Painter, and K. J. Vahala, "Ideality in a fiber-taper-coupled microresonator system for application to cavity quantum electrodynamics," *Phys. Rev. Lett.* **91**, 043902 (2003).
 30. V. S. Ilchenko, X. S. Yao, and L. Maleki, "Pigtailed high- Q microsphere cavity: a simple fiber coupler for optical whispering-gallery modes," *Opt. Lett.* **24**, 723–725 (1999).
 31. A. A. Savchenkov, I. S. Grudin, A. B. Matsko, D. Strekalov, M. Mohageg, V. S. Ilchenko, and L. Maleki, "Morphology-dependent photonic circuit elements," *Opt. Lett.* **31**, 1313–1315 (2006).
 32. A. A. Savchenkov, A. B. Matsko, and L. Maleki, "White-light whispering gallery mode resonators," *Opt. Lett.* **31**, 92–94 (2006).
 33. T. J. Kippenberg, S. M. Spillane, and K. J. Vahala, "Kerr-nonlinear optical parametric oscillation in an ultrahigh- Q toroid microcavity," *Phys. Rev. Lett.* **93**, 083904 (2004).
 34. A. A. Savchenkov, A. B. Matsko, D. Strekalov, M. Mohageg, V. S. Ilchenko, and L. Maleki, "Low threshold optical oscillations in a whispering gallery mode CaF_2 resonator," *Phys. Rev. Lett.* **93**, 243905 (2004).
 35. T. Carmon, H. Rokhsari, L. Yang, T. J. Kippenberg, and K. J. Vahala, "Temporal behavior of radiation-pressure-induced vibrations of an optical microcavity phonon mode," *Phys. Rev. Lett.* **94**, 223902 (2005).
 36. T. J. Kippenberg, H. Rokhsari, T. Carmon, A. Scherer, and K. J. Vahala, "Analysis of radiation-pressure induced mechanical oscillation of an optical microcavity," *Phys. Rev. Lett.* **95**, 033901 (2005).
 37. V. V. Vassiliev, V. L. Velichansky, V. S. Ilchenko, M. L. Gorodetsky, L. Hollberg, and A. V. Yarovitsky, "Narrow-line-width diode laser with a high- Q microsphere resonator," *Opt. Commun.* **158**, 305–312 (1998).
 38. A. B. Matsko, A. A. Savchenkov, N. Yu, and L. Maleki, "Whispering-gallery-mode resonators as frequency references. I. Fundamental limitations," *J. Opt. Soc. Am. B* **24**, 1324–1335 (2007).
 39. M. L. Gorodetsky and I. S. Grudin, "Fundamental thermal fluctuations in microspheres," *J. Opt. Soc. Am. B* **21**, 697–705 (2004).
 40. F. L. Walls and J. R. Vig, "Fundamental limits on the frequency stabilities of crystal oscillators," *IEEE Trans. Ultrason. Ferroelectr. Freq. Control* **42**, 576–589 (1995).
 41. M. L. Gorodetsky and V. S. Ilchenko, "Thermal nonlinear effects in optical whispering-gallery microresonators," *Laser Phys.* **2**, 1004–1009 (1992).
 42. A. E. Fomin, M. L. Gorodetsky, I. S. Grudin, and V. S. Ilchenko, "Nonstationary nonlinear effects in optical microspheres," *J. Opt. Soc. Am. B* **22**, 459–465 (2005).
 43. T. J. Johnson, M. Borselli, and O. Painter, "Self-induced optical modulation of the transmission through a high- Q silicon microdisk resonator," *Opt. Express* **14**, 817–831 (2006).
 44. M. Daimon and A. Masumura, "High-accuracy measurements of the refractive index and its temperature coefficient of calcium fluoride in a wide wavelength range from 138 to 2326 nm," *Appl. Opt.* **41**, 5275–5281 (2002).
 45. A. Feldman, D. Horowitz, R. M. Waxler, and M. J. Dodge, "Optical materials characterization," National Bureau of Standards Tech. Note 993 (U.S. Government Printing Office, 1979).
 46. A. Smakula and V. Sils, "Precision density determination of large single crystals by hydrostatic weighing," *Phys. Rev.* **99**, 1744–1746 (1955).
 47. S. S. Todd, "Heat capacities at low temperatures and entropies of magnesium and calcium fluorides," *J. Am. Chem. Soc.* **71**, 4115–4116 (1949).
 48. S. Andersson and G. Backström, "Thermal conductivity and heat capacity of single-crystal LiF and CaF_2 under hydrostatic pressure," *J. Phys. C* **20**, 5951–5962 (1987).
 49. G. A. Slack, "Thermal conductivity of CaF_2 , MnF_2 , CoF_2 , and ZnF_2 crystals," *Phys. Rev.* **122**, 1451–1464 (1961).
 50. R. Srinivasan, "Elastic constants of calcium fluoride," *Proc. Phys. Soc. London* **72**, 566–575 (1958).
 51. K. S. Pitzer, W. V. Smith, and W. M. Latimer, "The heat capacity and entropy of barium fluoride, cesium perchlorate and lead phosphate," *J. Am. Chem. Soc.* **60**, 1826–1828 (1938).
 52. D. T. Morelli and J. Heremans, "Thermal conductivity of single-crystal barium fluoride," *J. Appl. Phys.* **63**, 573–574 (1988).
 53. M. O. Manasreh and D. O. Pederson, "Elastic constants of barium fluoride from 300 to 1250 K," *Phys. Rev. B* **31**, 3960–3964 (1985).
 54. G. Ghosh, "Handbook of thermo-optic coefficients of optical materials with applications," (Academic, 1998).
 55. S. M. Etzel, A. H. Rose, and C. M. Wang, "Dispersion of the temperature retardance in SiO_2 and MgF_2 ," *Appl. Opt.* **39**, 5796–5800 (2000).
 56. A. Duncanson and R. W. H. Stevenson, "Some properties of magnesium fluoride crystallized from the melt," *Proc. Phys. Soc. London* **72**, 1001–1006 (1958).
 57. M. J. Dodge, "Refractive properties of magnesium fluoride," *Appl. Opt.* **23**, 1980–1985 (1984).
 58. J. D. Beasley, "Thermal conductivities of some novel nonlinear materials," *Appl. Opt.* **33**, 1000–1003 (1994).

59. I. H. Malitson, "Refraction and dispersion of synthetic sapphire," *J. Opt. Soc. Am.* **52**, 1377–1379 (1962).
60. W. M. Yim and R. J. Paff, "Thermal expansion of AlN, sapphire, and silicon," *J. Appl. Phys.* **45**, 1456–1457 (1974).
61. D. A. Ditmars, S. A. Ishihara, S. S. Chang, G. Bernstein, and E. D. West, "Enthalpy and heat-capacity standard reference material—synthetic sapphire (α -Al₂O₃) from 10 to 2250 K," *J. Res. Natl. Bur. Stand.* **87**, 159–163 (1982).
62. T. Toyoda and M. Yabe, "The temperature dependence of the refractive indices of fused silica and crystal quartz," *J. Phys. D* **16**, L97–L100 (1983).
63. T. H. K. Barron, J. F. Collins, T. W. Smith, and G. K. White, "Thermal expansion, Gruneisen functions and static lattice properties of quartz," *J. Phys. C* **15**, 4311–4326 (1982).
64. E. D. Palik, *Handbook of Optical Constants of Solids* (Academic, 1998).
65. C. Audoin, "Frequency metrology," in *Proceedings of the International School of Physics "Enrico Fermi," Course LXVIII*, A. F. Milone and P. Giacomo, eds. (North-Holland, 1980), pp. 169–222.
66. V. B. Braginsky and S. P. Vyatchanin, "Gravitational waves and limiting stability of self-excited oscillators," *Sov. Phys. JETP* **74**, 828–832 (1978).
67. V. B. Braginsky, "Experiments with probe masses," *Proc. Natl. Acad. Sci. U.S.A.* **104**, 3677–3680 (2007).
68. S. Biernacki and M. Scheffler, "Negative thermal expansion of diamond and zinc-blende semiconductors," *Phys. Rev. Lett.* **63**, 290–293 (1989).
69. K. Shimamura, H. Sato, A. Bensalah, V. Sudesh, H. Machida, N. Sarukura, and T. Fukuda, "Crystal growth of fluorides for optical applications," *Cryst. Res. Technol.* **36**, 801–813 (2001).
70. A. W. Sleight, "Isotropic negative thermal expansion," *Annu. Rev. Mater. Sci.* **28**, 29–43 (1998).